

HOT FORGING OF BIOMEDICAL B-Ti ALLOY STRENGTHENED BY HIGH OXYGEN CONTENT

Dalibor PREISLER, Josef STRÁSKÝ, Robert KRÁL, Miloš JANEČEK

Charles University in Prague, Faculty of Mathematics and Physics, Department of Physics of Materials, Ke Karlovu 5, 121 16, Praha 2, Czech Republic, EU, preisler.dalibor@gmail.com

Abstract

Beta titanium alloy, Ti-35Nb-6Ta-7Zr-0.7O (wt.%), differs from most of Ti-Nb-Zr-Ta based biomedical alloys by its very high oxygen content, which provides a significant interstitial solution strengthening. However, there is a need for thermomechanical processing due to the poor fatigue resistance after casting. This is caused by a residual porosity in the ingot and large grains (size > 1 mm). Die forging was used to work the cast rod with diameter of 45 mm into rods with diameters of 35 mm and 25 mm. Resulting microstructure and mechanical properties are evaluated and discussed. Heavily deformed microstructure with deformation bands is found in the 35 mm rod without apparent grain refinement. Further forging to 25 mm leads to recrystallization and significant refinement of grain size. Porosity observed in cast condition is removed by thermomechanical processing. Yield and tensile strength are improved while the fatigue performance remains low.

Keywords: Beta titanium, biocompatibility, die-forging, tensile testing, fatigue testing

1. INTRODUCTION

β -Ti alloys are promising group of materials for endoprostheses manufacturing mainly due to their excellent biocompatibility, when suitable alloying elements are used [1]. They have generally low Young's modulus, that is convenient for avoiding the so-called stress-shielding effect [2], that arises when rigid implant absorbs the mechanical loading [3] and the unloaded surrounding bone atrophies. The composition of β -Ti alloys, namely the oxygen content can significantly affect the Young's modulus and strength of the material [4-7].

The alloy Ti-35.3Nb-6.7Ta-7.3Zr-0.7O (wt.%) exhibits Young's modulus of 80 GPa [8] and its yield strength in as-cast condition is 900 MPa [9]. This high strength is caused mainly by high content of interstitial oxygen (0.7%), pinning the dislocations and thus strengthening the material [10]. However, the material in the as-cast condition is not suitable for implant manufacturing due to porosity and very large grain size (0.5 mm - 2 mm), that cause low fatigue performance. Therefore, the thermomechanical processing has to be performed.

2. MATERIAL AND METHODS

The initial Ti-35.3Nb-6.7Ta-7.3Zr-0.7O was cast at the company Retech Systems LLC. Ti and Zr sponge, Nb and Ta pieces and TiO₂ powder were melted by plasma arc melting into 2 kg compacts. These compacts were subsequently remelted in pure He atmosphere by sequential pour melting process to achieve the rod with the diameter of 45 mm.

Two rods with diameter 35 mm and 25 mm were produced by die-forging at the company ALPER a.s., Prostějov. Initial material after casting was heated approx. to 1200 °C in furnace in air (heating took approx. 20 min). The heated pieces were subsequently forged to 35 mm diameter in several steps using semi-constrained die and hydraulic press. The process took approx. 1 min and despite the forging die was pre heated to 300°C, the cooling of the material during processing (to approx. 900 °C) is unavoidable. The forged rods were cooled in water after forging. One of the forged pieces was reheated back to 1200 °C in furnace and forged to diameter 25 mm. During forging of the second piece, the temperature dropped below approx. 800 °C and this piece had to be reheated again. The piece with diameter 25 mm was finally also water quenched.

Samples for microstructural observations were made from central part of 35 mm rod and from both center and longitudinal edge of 25 mm rod. Scanning electron microscopy (SEM) observations and electron back-scatter diffraction (EBSD) measurements were conducted using microscope FEI Quanta 200F (FEG), operating at 10 kV for back-scattered electrons (BSE) observations and at 20 kV for EBSD measurements.

Round samples for tensile testing were machined from the rods to gauge diameter of 3 mm and length of 15 mm. Tensile testing was done with strain rate of 10^{-4} s^{-1} . Samples for fatigue testing had typical hourglass shape with diameter of 3 mm in the narrowest part. Fatigue testing was done in tension-compression test with $R = -1$.

3. RESULTS AND DISCUSSION

Figure 1a) shows microstructure of 35 mm rod. Note that porosity from casting [9] has been removed already in this condition. The grains did not undergo significant refinement during forging, their size remains in scale of 0.5 mm - 2 mm, but the band-like structure inside of them is evidence of deformation and formation of slip bands. However, this deformation is not homogeneous and some grains contain much less of these bands than the others. Example of such grain is in **Figure 1b)**. The channeling contrast in a large grain interior changes continuously, indicating only minor imposed strain. Similar microstructure behavior was found in whole cross-section with no big differences on the edge and in the center.

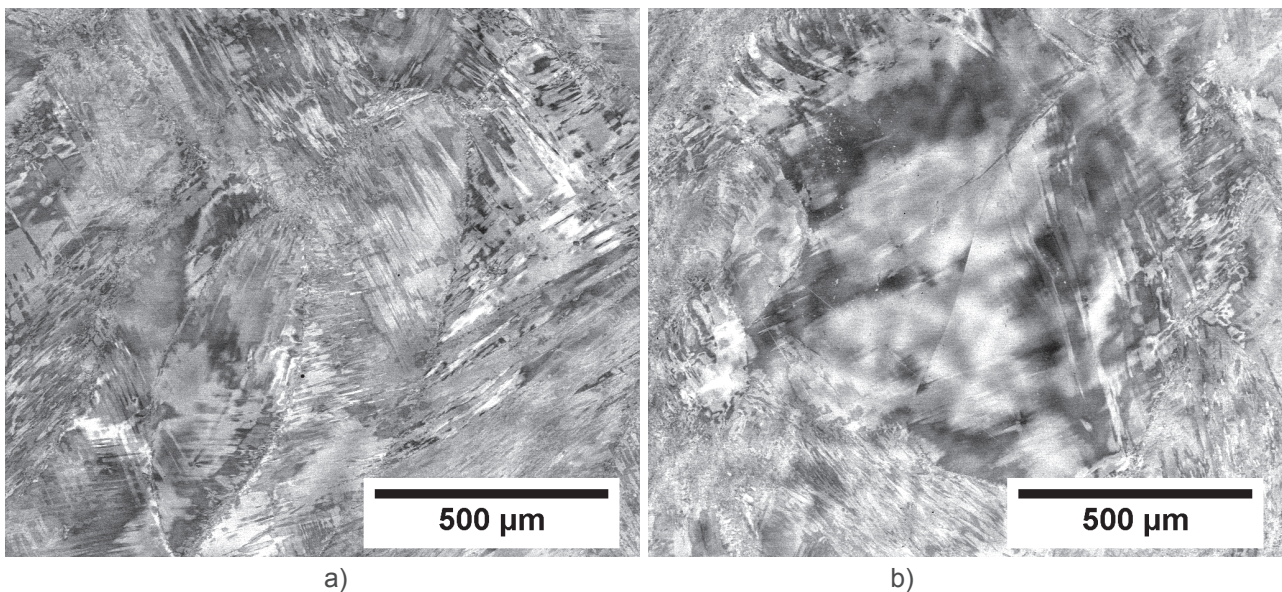


Figure 1 Microstructure (BSE) of 35 mm forged rod: a) overview, b) example of non-deformed grain

In the 25 mm rod, the deformation in the material is too high for observations by BSE. It is therefore necessary to employ the EBSD technique to characterize the microstructure. To measure the overall deformation present in each grain, grain orientation spread (GOS) can be computed from EBSD data. GOS is a characteristic angle for every grain and is calculated as an average misorientation between all measured points in a single grain and a mean orientation of the grain.

GOS maps from rod forged to 25 mm from longitudinal edge and center are shown in **Figures 2a)** and **2b)**, respectively. Note that the scale bar is ten times smaller than in the case of images of 35 mm rod. The edge contains equiaxed grains with the size around 50 µm. In the center of the rod, the grains are smaller than on the edge with the grain size around 20 µm. Significant grain refinement probably occurred during multiple heating of the rod between the two deformation steps. The deformed structure recrystallized while forming much smaller grains.

The cause of enhanced grain refinement in the center is surely higher deformation in this part of the rod, since there are higher values of GOS present in the center. Grain elongation is caused by deformation of previously recrystallized grains.

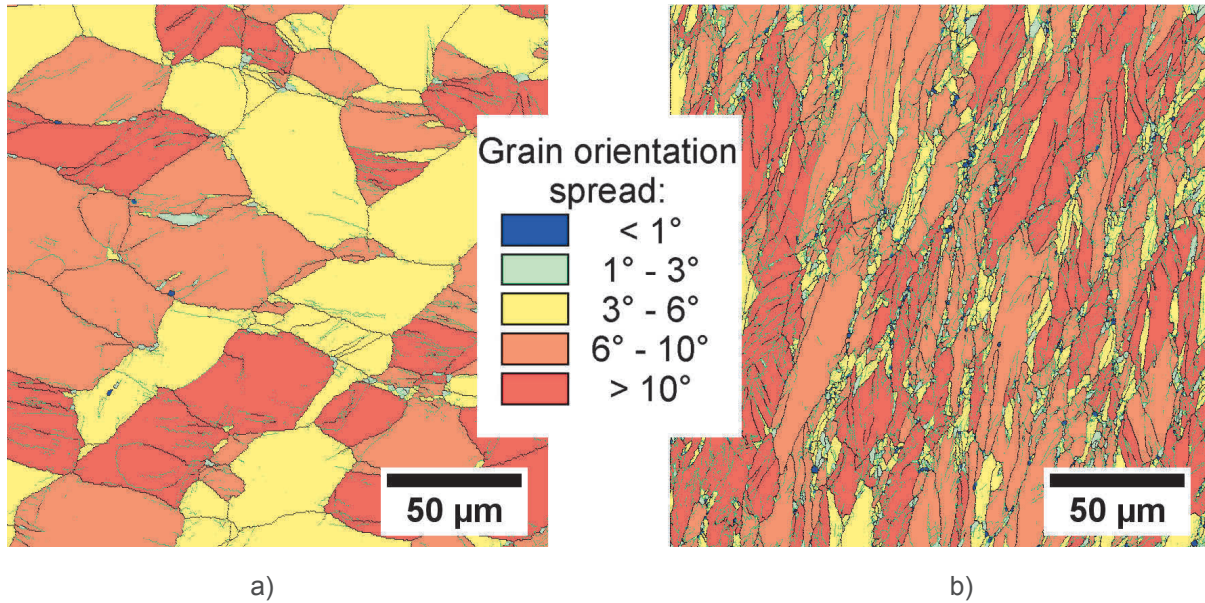


Figure 2 EBSD maps of 25 mm forged rod: a) longitudinal edge, b) center

The microstructural inhomogeneity of forged material resulted in significantly inhomogeneous mechanical properties. Mean yield stress (YS), ultimate tensile stress (UTS) and elongation are provided in **Table 1** along with comparatively high standard deviations. Representative flow curves from each metallurgical condition are shown in **Figure 3a**). The differences in the YS are large, systematic and significant in spite of large statistical error. Sharp yield point is more pronounced in the forged rods due to higher dislocation density introduced during deformation that causes more progressive pinning by oxygen atoms. The three flow curves differ in fracture mode. The cast material undergoes sudden brittle fracture while in forged material, the necking occurs. In the 25 mm rod, work hardening during tensile test is reduced due to the previous deformation and consequently the neck is formed at lower strains than in the 35 mm rod.

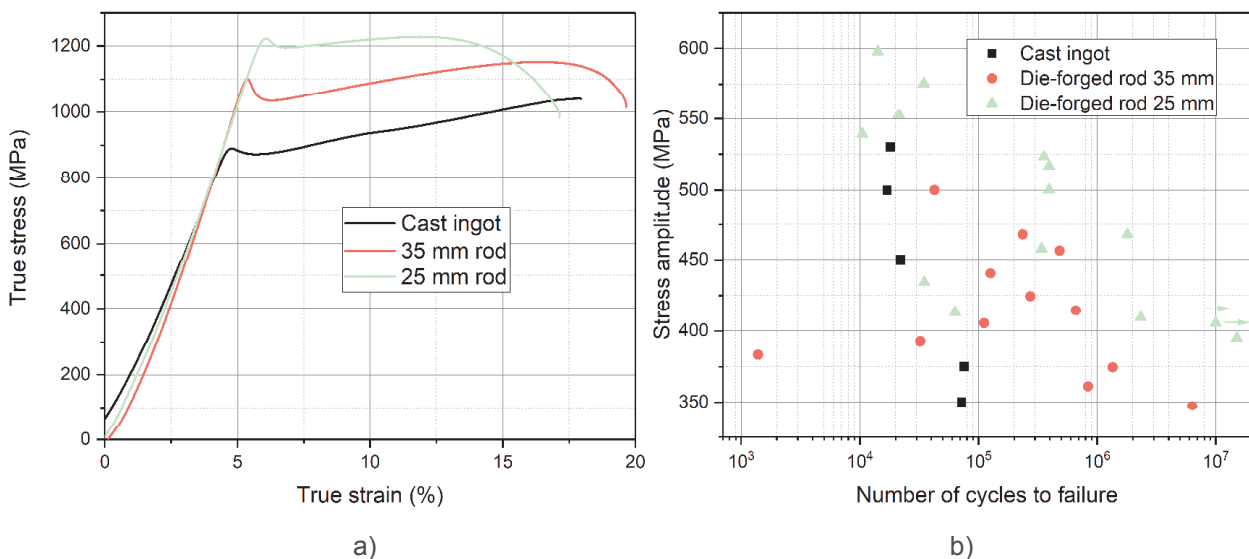


Figure 3 Mechanical properties of cast ingot and forged rods: a) Flow curves, b) S-N plot

S-N plot in **Figure 3b)** shows fatigue performance of both die-forged conditions along with data from the cast ingot. Again, significant inhomogeneity of mechanical properties due to microstructural inhomogeneity resulted in serious differences of performance of individual samples, which complicates overall assessment of fatigue endurance. Despite 35 mm rod shows improved fatigue resistance to cast ingot, it is still considered poor. The 10 million cycles to failure were not reached even at stress amplitude as low as 350 MPa. The low fatigue strength is most probably caused by initiating fracture on large grains in an inhomogeneous grain structure. Porosity removal clearly played only minor role in enhancing fatigue performance. The inhomogeneity of fatigue performance was large also in the 25 mm rod, but the overall endurance is better. The fatigue limit is estimated to be in range 350 MPa - 400 MPa.

Summary of achieved mechanical properties is shown in **Table 1**. Large errors of the tensile properties are caused by the aforementioned differences among individual samples. Both tensile properties and fatigue properties clearly improved by hot die-forging, however fatigue endurance is not sufficient for intended application of hip implant manufacturing.

Table 1 Summary of mechanical properties of cast and die-forged Ti-35.3Nb-6.7Ta-7.3Zr-0.7O alloy

	Yield strength (MPa)	Ultimate tensile strength (MPa)	Plastic strain to fracture (%)	Fatigue limit (MPa)
Cast ingot	870 ± 25	1039 ± 38	13.8 ± 1.7	< 350
Die-forged rod - 35 mm	1053 ± 71	1129 ± 76	14.1 ± 2.9	< 350
Die-forged rod - 25 mm	1256 ± 68	1264 ± 62	10.4 ± 2.0	~ 350 - 400

4. CONCLUSION

The β -Ti alloy with composition Ti-35.3Nb-6.7Ta-7.3Zr-0.7O (wt.%) was successfully die-forged after casting. Following conclusion can be drawn from presented results:

- Hot die forging removes porosity, induces plastic deformation and causes recrystallization in Ti-35.3Nb-6.7Ta-7.3Zr-0.7O alloy.
- Die-forging increases Yield strength and Ultimate tensile strength by work hardening, porosity removal and grain refinement. Ductility of 35 mm rod is comparable to the cast condition while the ductility of 25 mm rod is lower.
- The fatigue performance remains poor even after die-forging. Removing porosity itself did not provide significant improvement of fatigue properties. Homogeneous grain refinement is also required as indicated by results from 25 mm rod.

ACKNOWLEDGEMENTS

Financial support by the Ministry of Industry and Trade, project no. FV20147 is greatly acknowledged. DP acknowledges financial support by the Grant Agency of Charles University, project no. 1530217.

REFERENCES

- [1] EISENBARTH, E., VELTEN, D., MÜLLER, M. et al. Biocompatibility of β -stabilizing elements of titanium alloys. *Biomaterials*. 2004, vol. 25, pp. 5705-5713.
- [2] NIINOMI, M. Mechanical biocompatibilities of titanium alloys for biomedical applications. *Journal of the Mechanical Behavior of Biomedical Materials*. 2008. vol. 1, pp. 30-42.
- [3] SUMNER, D.R. Long-term implant fixation and stress-shielding in total hip replacement. *Journal of Biomechanics*. 2015. vol. 48, pp. 797-800.

- [4] FURUTA, T., KURAMOTO, S., HWANG, J. et al. Mechanical properties and phase stability of Ti-Nb-Ta-Zr-O alloys. *Materials Transactions*. 2007. vol. 48, pp. 1124-1130.
- [5] WEI, Q., WANG, L., FU, Y. et al. Influence of oxygen content on microstructure and mechanical properties of Ti-Nb-Ta-Zr alloy. *Materials & Design*. 2011. vol. 32, pp. 2934-2939.
- [6] QAZI, J.I., RACK, H.J. and MARQUARDT, B. High-strength metastable beta-titanium alloys for biomedical applications. *JOM*. 2004, vol. 56, pp. 49-51.
- [7] NAKAI, M., NIINOMI, M., AKAHORI, T. et al. Effect of oxygen content on microstructure and mechanical properties of biomedical Ti-29Nb-13Ta-4.6Zr alloy under solutionized and aged conditions. *Mater. Trans.* 2009. vol. 50, pp. 2716-2720.
- [8] STRÁSKÝ, J., HARCUBA, P., VÁCLAVOVÁ, K. et al. Increasing strength of a biomedical Ti-Nb-Ta-Zr alloy by alloying with Fe, Si and O. *Journal of the Mechanical Behavior of Biomedical Materials*. 2017. vol. 71, pp. 329-336.
- [9] PREISLER, D., VÁCLAVOVÁ, K., STRÁSKÝ, J. et al. Microstructure and mechanical properties of Ti-Nb-Zr-Ta-O biomedical alloy. In *METAL 2016: 25rd International Conference on Metallurgy and Materials Ostrava: TANGER*, 2016. pp. 1509-1513.
- [10] GENG, F., NIINOMI, M. and NAKAI, M. Observation of yielding and strain hardening in a titanium alloy having high oxygen content. *Materials Science and Engineering: A*. 2011. vol. 528, pp. 5435-5445.